Development of the Advanced T-OZON$_{TM}$ for PWR Decommissioning – 16062

Koji Negishi*, Yumi Yaita*, Masato Okamura*,
Toshihiro Yoshii*, Yasushi Yamamoto*, Satoru Abe*,
Taro Kanamaru*, Hiromi Aoi*, Akira Ikeda*
Neil Swift**, Darik Tippetts**, Randy Duncan**
*Toshiba Corporation
**Westinghouse Electric Company

ABSTRACT
T-OZON$_{TM}$ is the chemical decontamination method developed by Toshiba for the decontamination of BWR system piping. To apply T-OZON$_{TM}$ to PWR decommissioning, the decontamination application conditions have been optimized on actual PWR plant samples and ozone concentration behavior in the water have been studied.

INTRODUCTION
The numbers of aging nuclear power plants slated for closing have increased around the world. The majority of them are PWRs. It would be desirable for a chemical decontamination method to reduce the exposure of PWR decommissioning workers. Toshiba had developed T-OZON$_{TM}$ that was a chemical decontamination method for BWRs [1, 2, 3]. The method has been applied more than 90 times in Japanese BWR plants to date. The radiation exposure reduction of workers by applying T-OZON$_{TM}$ is estimated at about 300-2700 man mSv [4]. A major feature of T-OZON$_{TM}$ is the reduced amount of radioactive waste produced when compared to other decontamination processes.The oxide film on PWR wetted surfaces is harder to decontaminate than that of a BWR due to its chemical composition. To apply the T-OZON$_{TM}$ to PWR oxide films, it is necessary to adapt the process application conditions. The behavior of the decontamination agent, ozone, was important to model for the full system decontamination. Ozone is self-decomposable substance and it was important to determine the optimal ozone injection conditions to maintain the dissolved ozone concentration in a large system.
In this study, the decontamination application parameters and behavior of ozone were examined by initially performing dissolution tests on coupons with simulated oxide films and the application parameters were used to decontaminate actual PWR samples. The behavior of ozone was simulated with a new model which considered the dissolution of ozone in PWR systems. This model was incorporated into the model for the simulation of BWR full system decontamination [5].

IMPROVEMENT OF DECONTAMINATION CONDITIONS
(1)Principle of T-OZON$_{TM}$
Currently, most of chemical decontamination methods use an oxidizing agent and a reducing agent. T-OZON$_{TM}$ uses ozone as the oxidizing agent and oxalic acid as the reducing agent. The principle of T-OZON$_{TM}$ is shown in Fig.1. Reductive dissolution of

iron oxide by oxalic acid and oxidative dissolution of chromium oxide by ozone are conducted alternatively. In the case of BWR oxide films, the number of times of reduction step is many more than that of oxidation step because iron oxide is main constituent in the film. As shown in Fig.2, first cycle is reduction step. After the first cycle, each cycle contains the oxidation step and the reduction step. Combination cycle is repeated up to 2 times (Fig.2).
Decontamination Factors greated than 100 (DF =activity before decontamination / activity after decontamination) have been obtained in the component decontamination such as RRS pump internals and DF 10 ~ 40 have been obtained in system decontaminations.
Ozone is self-decomposable substance and oxalic acid can be decomposed by ultraviolet light and hydrogen peroxide.
Phosphoric acid used in the oxidation step for pH adjustment is source of slight waste. The radioactive waste generation due to the decontamination agents is small.

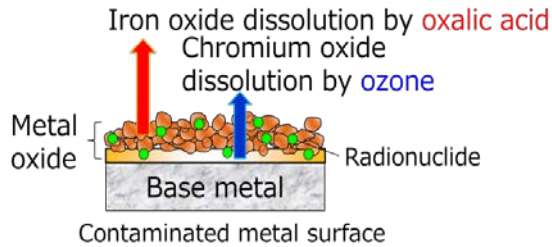

Fig.1 Principle of T-OZON$_{TM}$

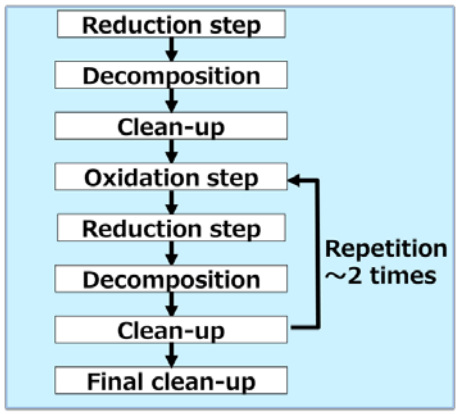

Fig.2 T-OZON$_{TM}$ Procedure

(2)Characteristics of PWR oxide film

Reactor water conditions of PWR and BWR are shown in Table.1. A feature of PWR reactor water is high dissolved hydrogen concentration and low dissolved oxygen concentration compared to BWR. Namely, it is a reductive water condition. In such circumstance, the chromium oxide grows thicker than in BWR [6]. In addition, Steam generator (SG) tube in PWR causes high percentage of nickel-based alloy in the primary system structural material. The outer layer oxide of nickel-based alloy is composed of nickel rich oxides [7, 8] that have low solubility in the decontamination solution. Fig.3 shows comparison of oxide composition in PWR and BWR. For applying T-OZON$_{TM}$ to a PWR, it is necessary to strengthen the oxidation ability to dissolve thick chromium oxide and it is also necessary to optimize the reduction condition to remove the nickel rich oxide. This testing examined the potential of the decontamination solution in order to make these improvements.

Table.1 Typical reactor water conditions of PWR and BWR

	PWR	BWR
DH (ppb)	3000	50
DO (ppb)	< 5	10 – 200
Temp. (°C)	310	285
Li (ppm)	5	-
B (ppm)	100-2000	-
Zn (ppb)	>20	0-5

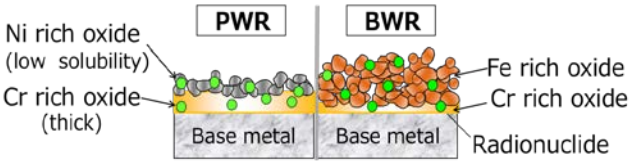

Fig.3 Schematic diagram of PWR and BWR oxide composition

(3)Oxide and metal dissolution test

Under PWR reductive conditions, oxide growth is very slow. It is difficult to form the oxide on metal under PWR simulated conditions in a short time in the laboratory. Therefore, in the dissolution testing, oxide was grown on metal under BWR simulated conditions and oxide reagents. For strengthening of the oxidation ability, it is necessary to increase the redox potential of the decontamination solution by increasing the dissolved ozone concentration. In order to increase the dissolved ozone concentration, it is effective to suppress the self-decomposition of ozone under acidic condition. However, a large amount of acidic additives creates a large amount of secondary wastes. Nitric acid was selected as an additive for pH control that does not increase secondary waste more than is typical for a BWR. The effect on oxide solubility by increasing the dissolved ozone concentration and redox potential was examined by controlling the pH using nitric acid. Chromium oxide that dissolves in the oxidation step can be formed even under BWR water condition. Oxide dissolution properties are possible to ascertain using oxide grown under BWR conditions. Type304 stainless steel test specimens which were pre-filmed for 3000 hours in BWR primary system water condition were used. After 2 hours immersion in 80 °C ozone solution, test specimens were immersed for 1 hour in 95 °C, 2000ppm oxalic acid. After immersion, the specimens were washed with pure water, dried and weight was measured. The weight loss of the specimens was due to oxide dissolution amount. Fig.4 shows the results. It should be noted that in the present paper, decontamination solution potential mV indicates the value that was measured by the Ag/AgCl electrode and 3.3MKCl electrolyte. The potential of the decontamination solution and dissolved oxide amount increased by increasing the dissolved ozone concentration. In the decontamination of a BWR, dissolved ozone concentration is usually around 1 ppm. If the dissolved ozone concentration reaches 5 ppm, oxide dissolution amount increases 1.5 times or more.

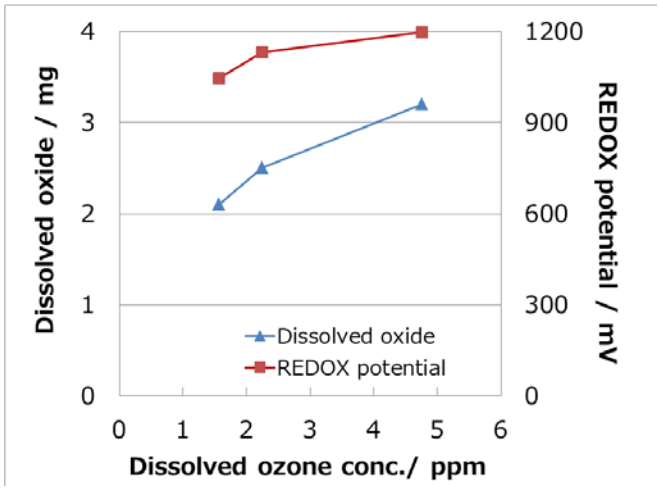

Fig.4 Effect of dissolved ozone for oxide dissolution

As alternatives of nickel rich oxide, nickel ferrite powder was used to clarify the effect on the solubility by the REDOX potential of the oxalic acid solution. Oxalic acid solution was 95 ℃ at the concentration of 2000 ppm and was added iron of 20ppm. Control of REDOX potential was done by UV irradiation due to control Fe^{2+} / Fe^{3+} concentration ratio. Nickel ferrite powder was added into the solution and immersed in 2 hours. After the immersion, the concentration of dissolved nickel in the solution was analyzed to calculate the nickel ferrite dissolution amount. The results are shown in Fig.5. Natural potential of oxalic acid solution was about 200mV. Dissolution of nickel was increased along with the potential drop. At the negative potential conditions, nickel ferrite solubility showed about three times the solubility in the natural potential.

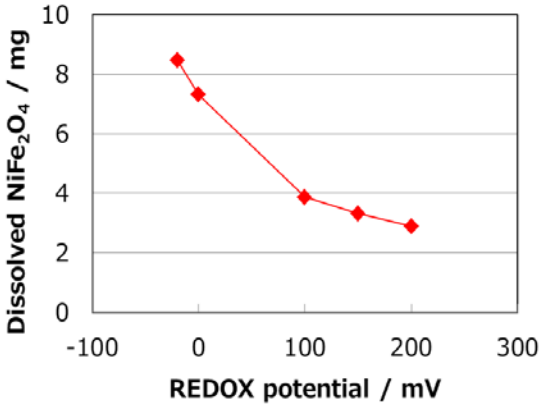

Fig.5 Effect of REDOX potential of oxalic acid for nickel ferrite dissolution

The metal dissolution tests were carried out using test specimen of type304 stainless steel, nickel-based alloy 600 at varying the potential of oxalic acid solution. As with the nickel ferrite powder dissolution test, 95 ℃, 2000ppm of oxalic acid, and controls the solution potential by ultraviolet irradiation at 20ppm iron addition, metal specimens were immersed 2 hours. After picking up from the solution, the test specimens were washed dried and weight was measured. The weight loss was regarded as a metal dissolved amount. As shown in Fig.6, the SS304 and Alloy600 showed the reverse tendency of solubility depended on the solution potential. The best potential for metal dissolution was different depending on the material. Dissolution amount of each metal by the potential control was improved by about 4-5 times. However, dissolution of the excess base metal increases the secondary waste generation. We must consider the optimal decontamination condition for achieving the required decontamination ability and small secondary waste.

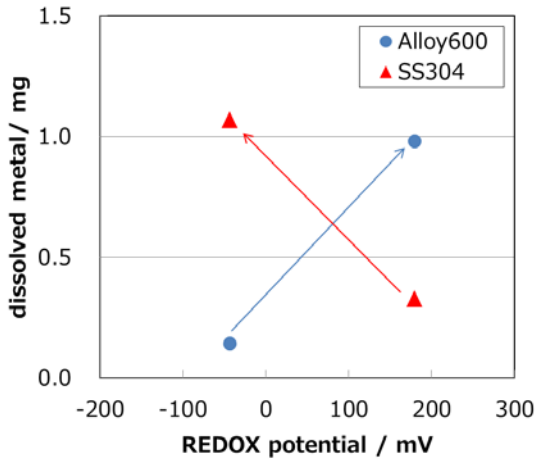

Fig.6 Effect of REDOX potential of oxalic acid for base metal dissolution

From the above cold test study about chromium oxide, nickel rich oxide, base metal, decontamination conditions were found to be able to improve the solubility of each material. In the next section, decontamination test of actual PWR sample was conducted based on this result for confirmation of decontamination effect.

(4) Decontamination test

Decontamination tests by using contaminated samples were conducted to confirm that the Advanced T-OZON$_{TM}$ process had sufficient effect. The samples were tube made of alloy 600 TT and structure material made of stainless steel at Steam Generator removed from PWR plants in USA. The goal of decontamination performance was postulated to be a decontamination factor (= activity before decontamination / activity after decontamination) of 30. One cycle of decontamination test contains oxidation step and reduction step. In these tests, combination cycle was repeated up to 3 times. Test conditions of each step were shown as Table. 2 Regarding stainless steel, value of ORP was lower than 0 mV by UV irradiation. While regarding alloy 600 TT, value of ORP was lower than 0 mV by UV irradiation at 1st step. From 2nd cycle, value of ORP was changed more than 100 mV without UV irradiation to prompt dissolution of base metal. The Summary about samples before and after tests is shown as Table.3 and the results of DF are shown as Fig.7. According to these results, it could be confirmed that DF achieved more than 30 as our goal within 3 cycles and advanced T-OZON$_{TM}$ process had a competent performance for decontamination of PWR.

Table.2 Test conditions

	Oxidation step	Reduction step
Temp. (°C)	80	95
pH (-)	3.0	2.0
Dis. O_3 (ppm)	3.0<	-
Oxalic acid (ppm)	-	2000

Table.3 The Summary about samples

			
Before test	After test	Before test	After test
Material: Stainless steel Contaminated area: 1.0cm^2 Initial ^{60}Co activity : 2.5×10^5 Bq/cm^2 Final ^{60}Co activity : 5.9×10^3 Bq/cm^2		Material: Alloy600TT Contaminated area: 8.0cm^2 Initial ^{60}Co activity : 1.6×10^4 Bq/cm^2 Final ^{60}Co activity : 3.8×10^2 Bq/cm^2	

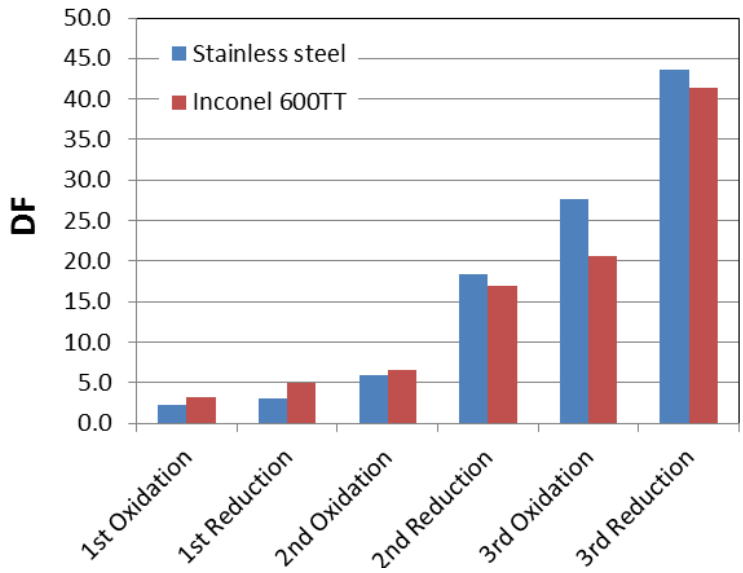

Fig.7 Results of DF

OZONE BEHAVIOR SIMULATION

To apply T-OZON$_{TM}$ to PWR system, the ozone concentration has to be evaluated in the system and some large components, such as the reactor vessel. Therefore, we have been developing the ozone concentration evaluation method.

(1) Experiment

(1-1) Objective

Ozone has been using for water treatment system. Many studies about behavior of dissolving ozone under liquid-gas two phase have been conducted. However, the most of these data were obtained at low temperature, because dissolved ozone into water is very easy to decompose. Regarding decontamination, temperature is very important factor, so decontamination has to be conducted under high temperature. Therefore, to get high DF, ozone concentration into water has to keep as high as possible and best condition about injecting ozone gas into PWR plant has to be investigated.

Generally, behavior of dissolving self- decomposable gas like ozone can be described by;

$$\frac{dC}{dt} = K_L \times a(C^* - C) - kC \quad (1)$$

Where K_L is the mass transfer coefficient, *a* is the total gas- liquid contact surface area per volume, C* is the equilibrium concentration of ozone, C is the ozone concentration, k is the decomposition rate, and t is time. According to many previous researches, k of ozone strongly depends on pH value and temperature. In our previous test, effect

of pH value and temperature on k of ozone under decomposition condition had been evaluated. The results are shown as Fig.8. But K_L and C* have not been evaluated yet. So in this study, the value of K_L and C* was evaluate by ozone Dissolution test under liquid-gas two phase at high temperature.

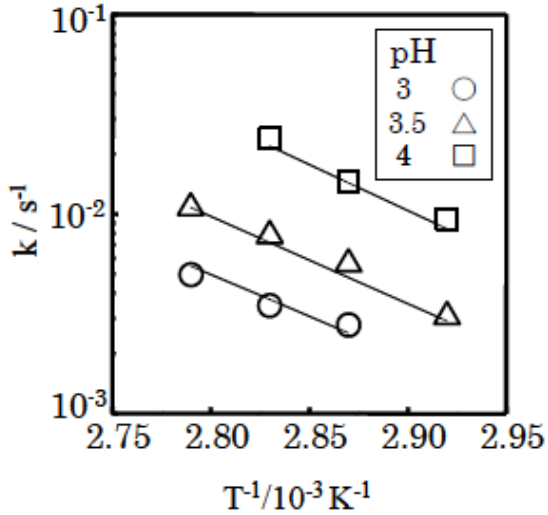

Fig.8 Relationship between k and pH and temperature

(1-2) Test loop

Schematic view of the test circulation loop is shown in Fig.9. To absorb as high concentration ozone gas into water as possible, the loop was provided with a multiphase pump for the transport of liquid-gas mixtures and for the enrichment of liquids with gases (Nikuni Turbo Mixer KTM Pump). Ozone was generated by Ozone-Generator (Iwasaki Electric OP-30W) and connected to KTM Pump to generate ozone-water two-phase flow. Gas ozone concentration at inlet was measured by ozone meter (Ebara-Jitsugyo EG-600). Before coming back the tank (volume; 20L), gas remaining without being dissolved into water was removed by gas-liquid separation tank and was decomposed by ozone decomposer before releasing to the atmosphere.

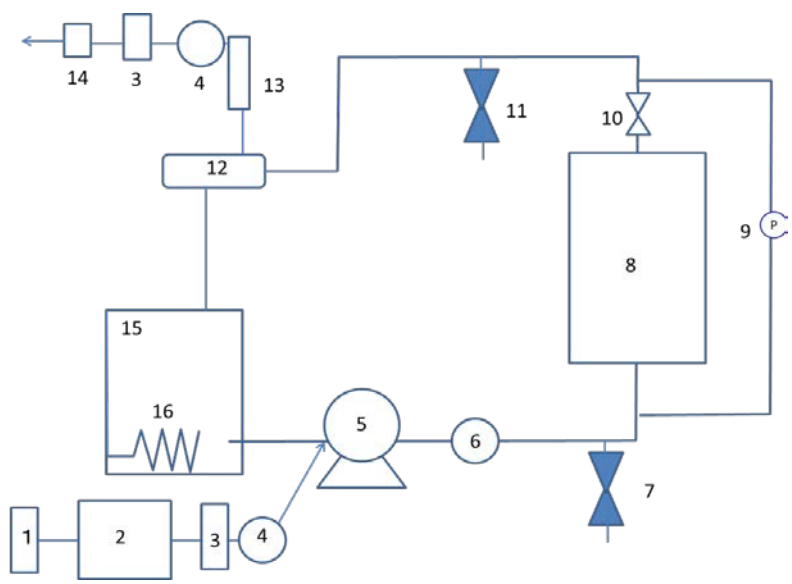

Fig.9 Schematic view of the test circulation loop

1:Oxygen gas holder, 2:Ozone generator, 3 : Gas phase Ozone meter, 4:Flow meter, 4:Cooler, 5: Multiphase pump, 6 : Flow meter, 7 : Sampling stopcock at inlet, 8:Test section, 9 : Differential pressure gauge, 10 :Valuve, 11 ; Sampling stopcock at outlet, 12 : Gas-liquid separation tank, 13:Cooler, 14: Ozone decomposer, 15:Tunk, 16: Heater

Temperature was increased by heater at the tank. Pressure was controlled by closing valve at outlet of test section. Flow rate can be adjusted by controlling inverter

frequency of pump. The main structural material for the test loop was Type 304 stainless steel. Two kind types of test sections were attachable according to the purpose of use. One type were having coiled flow path made of stainless steel. This was used for obtaining data about k_L andC*. This coiled type test secotions were three whose path length are 5 m,10 m and 15 m. Another type were having square path made of acrylic. This was used for measuring bubble size distribution for evaluating a (=the total gas- liquid contact surface area per volume).

(1-3) Bubble size distribution measuring test

In order to evaluate *a* (= the total gas- liquid contact surface area per volume), bubble size distribution was observed by using a high speed camera (Kato Koken K5). Schematic view of the measurement system is shown in Fig.10. Its system can record image at 8000 frames per second (fps) using 1280 × 1024 pixels. Flow rate was adjusted from 10 L/min to 20 L/min, gas flow rate was adjusted from 0.3 to 1.2 L/min and void fraction was adjusted from 0.03 to 0.06. Gas ozone concentaration was kept more than 100g/Nm^3. The ferret-diameter, X/Y ratio and projected area were calculated from image by flow analysis software (Kato Koken FlowExpert2D2C).

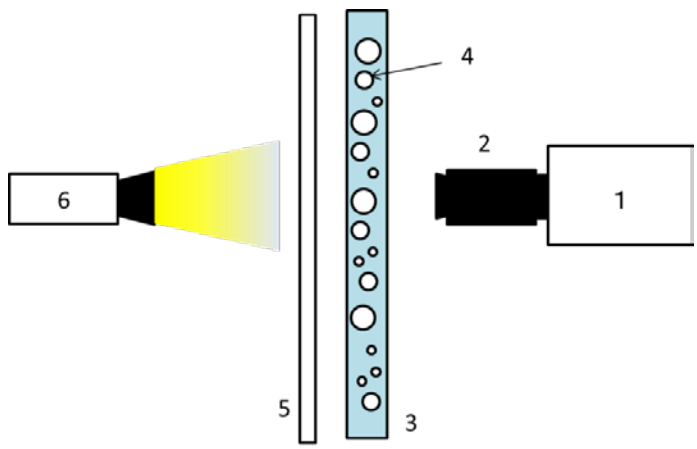

Fig.10 Measurement system for bubble size distribution

1:High speed camera, 2: Magnifying lens, 3 : Test section (made of acrylic), 4:Bubble, 5:Screen, 6 : Spot light

(1-4) Ozone Dissolution test

In order to evaluate K_L, ozone dissolution tests were conducted by using the test loop under simulated decontamination conditon. The pressure and temperature were kept at 0.4 MPa and 80 °C, respectively. Flow velocity was adjusted from 0.5 m/s to 1.0 m/s, path length was adjusted from 5 m to 15 m, gas flow rate was adjusted from 0.3 to 1.2 L/min and void fraction was adjusted from 0.03 to 0.06. Gas ozone concentaration was kept more than 100g/Nm^3. Until dissolved ozone concentration reached the saturation, dissolved ozone concentration was measured at every 3 minutes. After dissolved ozone concentration reached the saturation, dissolved ozone concentration was measured at every 5 - 10 minutes.The potassium iodide (KI) method was used for measuring dissolved ozone concentration.

(1-5) Result of Bubble size distribution

One of the binarized image of bubble size distribution is shown as Fig.11. Bubbles linking two or more were excluded from analysis. Bubble size were evaluated by calucating Heywod-diameter from flow analysis results. One of the histogram described Bubble size destribution as Heywod-diameter is shown as Fig.12. Generally, regarding reaction particle by evaporation, volatilization and dissolution, Sauter mean diameter (SMD) are used for evaluation. SMD is given by ;

$$SMD = \frac{\sum N_i x_i^3}{\sum N_i x_i^2} \quad (2)$$

Where N_i is number of particle, and x_i is particle size. In this study, the results of SMD was from 150 to 350 μm.

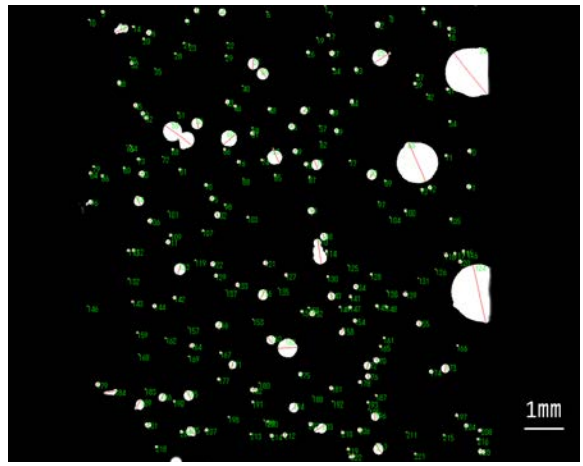

Fig.11 The binarized image of bubble size ditribution

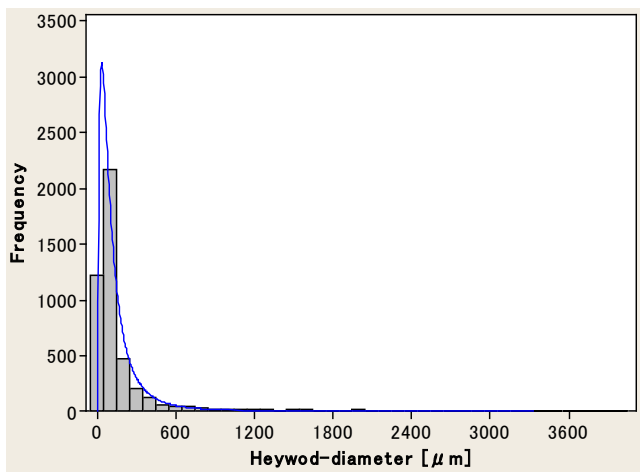

Fig.12 Histogram described Bubble size destribution as Heywod-diameter

(1-6) Result of Ozone Dissolution test

Dissolved ozone concentration can be described by Eq.(1). Integrating Eq. (1) yields

$$C = \frac{K_L \times a}{K_L \times a + k} \times C^*[1 - \exp\{-(K_L \times a + k) \times t\}] \quad (3)$$

When t = ∞, the dissolved ozone concentration can be described as saturated dissolved ozone concentration by Eq. (2).

$$C_\infty = \frac{K_L \times a}{K_L \times a + k} \times C^* \quad (4)$$

Where C_∞ is the saturated dissolved ozone concentration. Eq. (3) can be rewritten as follows;

$$log_{10}\left(\frac{C_\infty - C}{C_\infty}\right) = -\frac{K_L \times a + k}{2.303} \times t \quad (5)$$

Therefore, when plotting unsaturation rate (= C_∞-C / C_∞) against time on single logarithmic chart, if a and k are known, K_L can be calculated from slop of approximation straight line. One example of the results of ozone dissolution tests is shown as Fig.13. According to previous tests, in this test condition (pH=3.0, Temperature= 80 °C),value of k is 0.00347 s^{-1} and *a* (= the total gas- liquid contact surface area per volume) can be caluclated by results of bubble size(Range from 150 to 350 μm at SMD).As a result of evaluation, K_L was the range from 3.0×10^{-3} m/s to 3.0×10^{-2} m/s.

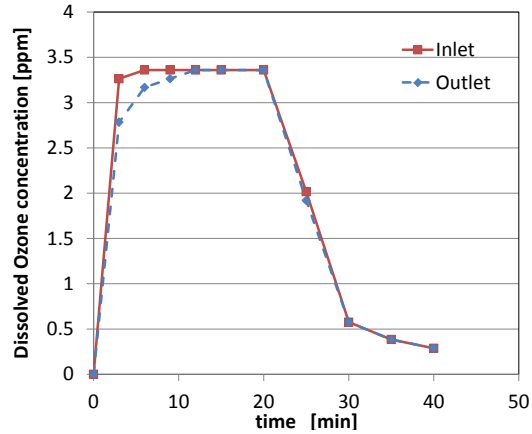

(a) Behavior of dissolved ozone

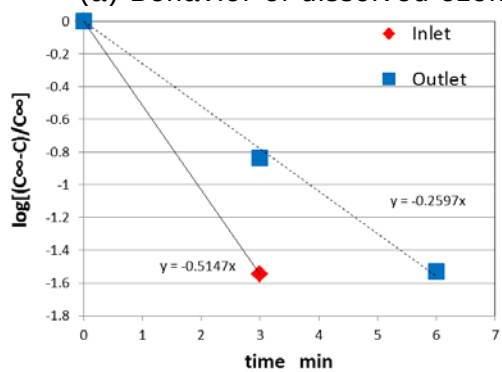

(b) Plotting unsaturation rate against time

Fig.13 One example of results of ozone dissolution

(2)Simulation result

At the development for BWR, only the self-decomposition of dissolved ozone had been considered. Now, new model considering the dissolution of the ozone from bubbles into water was added to the simulation model. To simulate the bubbly two-phase flow, Eulerian equation was applied. To calculate the ozone concentration in the water, the dissolution of ozone from bubbles and self-decomposition of ozone in the water were modeled as showed in Eq. (1). The decomposition rate k is 3.47×10^{-3} s^{-1}, saturation ozone concentration C_∞ is 3.44 ppm, and supposed the diameter of bubbles to be 200μm, we assumed the mass transfer coefficient K_L to be 1.476×10^{-3} m/s.

The test section geometry is shown in Fig.14. The number of the mesh was 2,420,000. Here, we simulated the dissolved ozone distribution in the water at 15 minutes of the examination, assuming a steady-state. Analysis condition is shown in Table.4. The ozone concentration of the inlet of the test section is 3.36 ppm, Flow rate is 10.38 L/min, gas flow quantity rate is 2.0 vol%.

The calculated results of the ozone concentration distribution in the test section with/without the dissolution model are shown in Fig.15. The calculated results of the ozone concentration with/without the dissolution model in the flow direction are shown in Fig.16. In Fig.16, triangle shows the experimental result of the ozone concentration at the exit of the test section.

The ozone concentration at the exit of test section without dissolution model is 3.03 ppm, and that of using dissolution model is 3.36 ppm. The ozone concentration at the exit of test section increases by applying dissolution model. Moreover, as shown in Fig.16, the ozone concentration at the exit of test section becomes close to the experimental result.

Table.4 Analysis condition

Temperature	80(°C)
Pressure	0.4(MPaG)
Flow rate (gas)	0.822(L/min) at 0.1MPa 0°C
Flow rate (liquid)	10.38(L/min)
Gas flow quantity rate	2(vol%)
Diameter of bubbles	200(μm)
Ozone concentration at inlet	3.36(ppm)

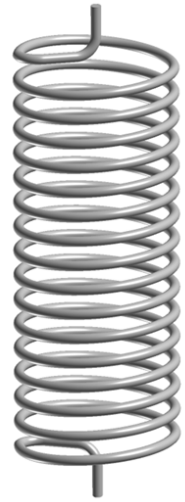

Fig.14 Test section geometry

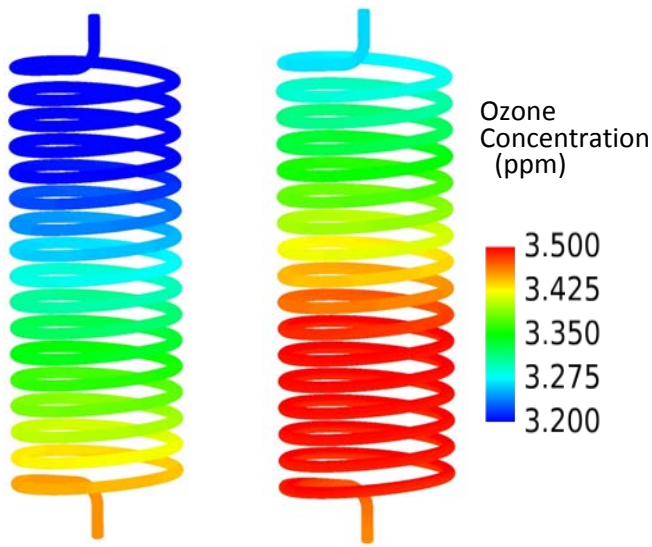

Without dissolution model

With dissolution model

Fig.15 Ozone concentration distribution in test section

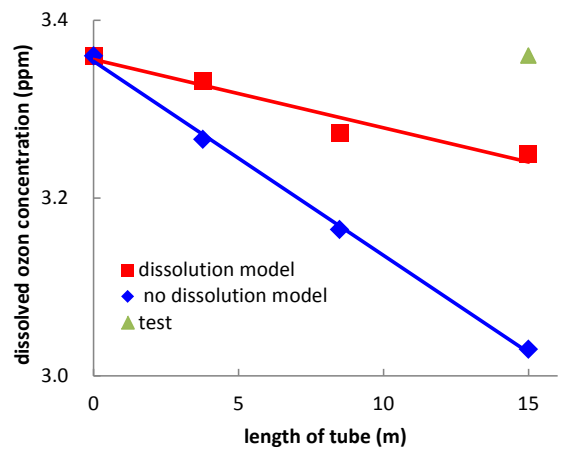

Fig.16 The comparison of the ozone concentration distribution in the flow direction with/without dissolution model

CONCLUSIONS

The Toshiba T-OZON$_{TM}$ chemical decontamination method is being improved for PWR decommissioning. This study is summarized as follows,

· Cold test results

The solubility of chromium oxide is high at high ozone concentration with high potential. The solubility of nickel rich oxide is good at low potential of oxalic acid solution. SS304 dissolved well at negative potential and alloy600 dissolved well at positive potential. The best potential for metal dissolution was different depending on the material.

·Decontamination testing

For actual PWR artifacts, decontamination tests were done. It was confirmed that the goal of reaching a DF of >30 within 3 cycles for SS304 and alloy600 could be achieved.

·Ozone behavior simulation

A new condition considering the dissolution of ozone into water was added to the simulation model. As a result, a close correlation of the model to the experimental results was obtained.

In the next study, optimization of conditions to enhance decontamination effectiveness, improvement of simulation accuracy and evaluation of ozone distribution in a PWR system will be performed.

REFERENCES

1. Y. Yaita et al.,"Chemical Decontamination Using Ozone Oxidation Process", Proc. of 9th Int. Conf. on Nuclear Engineering, ICONE9-1139 (2001)
2. M. Enda et al.,"Application of ozone chemical decontamination (T-OZON) to the equipments for disposal", Proc. of 10th Int. Conf. on Nuclear Engineering, ICONE10-22430 (2002)
3. Y. Yaita et al.,"Decontamination of BWR primary system by T-OZON process", Proc. of 11th Int. Conf. on Nuclear Engineering, ICONE11-36322 (2003)
4. Y. Yaita, "Development and Application of T-OZON process", Genshiryoku eye, Vol.50,No.5, p. 58-61(2004) (in Japanese)
5. N. Ichikawa et al., "Application of T-OZON process to reactor pressure vessel and its internals decontamination," Int. Conf. on Water Chemistry of Nuclear Reactor Systems", Vol. 2, Session4-4.3, (2006).
6. T. Terachi et al. , "Corrosion Behavior of Stainless Steels in Simulated PWR Primary Water – Effect of Chromium Content in Alloys and Dissolved Hydrogen- " Journal of Nuclear Science and Technology, 45, pp.975-984(2008)
7. T. Terachi et al. , "Influence of Dissolved Hydrogen on Structure of Oxide Film on Alloy 600 Formed in Primary Water of Pressurized Water Reactors" Journal of Nuclear Science and Technology, 40, pp.509-516 (2003)
8. S. Ranganathan et al. , "Comparative study on the dissolution behavior of Fe_3O_4,γ-Fe_2O_3 and $NiFe_2O_4$ in DCD formulation a mechanistic approach", 1st International Conference Water Chemistry of Nuclear Reactor Systems,

6:Proceedings London, British Nuclear Energy Society (BNES), pp.262-265 (1992)[i]

[i] T-OZON is the trademark of Toshiba corporation.